

Magnonic-Crystal Waveguides of Width-Modulated Thin-Film Nanostrip Applicable for Broad-Band Microwave Spin-Wave Filter

Ki-Suk Lee, Dong-Su Han, and Sang-Koog Kim*

*Research Center for Spin Dynamics & Spin-Wave Devices and Nanospinics Laboratory,
Department of Materials Science and Engineering, College of Engineering,
Seoul National University, Seoul 151-744, Republic of Korea*

We propose, by micromagnetic modeling and theoretical calculation, a novel planar structure of magnonic-crystal waveguides in which the allowed and forbidden bands of traveling dipolar-exchange spin-waves can be manipulated simply by means of the periodic modulation of different widths in thin-film nanostrips made of a single magnetic material. The periodic width modulation and its periodicity in the nanostrips are crucial parameters for controlling spin-wave band gaps of the order of ~ 10 GHz. A new type of magnonic crystals of combinations of the differently strip-width modulated nanostrips in serial provides a route to the realization of broad-band spin-wave filters in a high frequency range above ~ 10 GHz.

Over the past decade, photonic crystals [1] have been a hot topic in the research fields of condensed matter physics and optics, owing to their various applications to optical nano-devices such as photonic waveguides [2] and integrated circuits [3]. Meanwhile, in the research areas of nanomagnetism and magnetization \mathbf{M} dynamics, the magnetic counterpart of the photonic crystal, the so-called magnonic crystals (MCs), are also of growing interest, owing to their applications to spin-wave (SW) devices such as waveguides and filters [4]. In recent years, a lot of theoretical and experimental studies have been conducted on not only various types of MCs including one-dimensional (1D) structures such as periodic multilayers [5,6], periodic arrays of nanostrips [7], corrugated films [8,9], and comb-like [10] or serial loop structures [11], but also including 2D or 3D structures [12,13,14]. In such structures, the allowed and forbidden SW modes (called magnons) are controllable by means of the artificial periodic structure of magnetic media having different magnetic properties, such as magnetic material parameters [5,6,15], shape [8,9,10,11] and exchange-biased field [16]. Despite recent advances in fundamental understandings of those MCs as well as the wave properties of excited SW modes, few studies have been carried out on simple structures of MC waveguides for practical applications to broad-band spin-wave filters. Very recently, it has been demonstrated experimentally that 20 ~ 40 MHz wide band gaps of magnetostatic SWs can be controlled by means of periodic shallow grooves (a few tens of μm width and a few hundreds nm depth) etched on an yttrium iron garnet film [9]. However, for future SW-based signal process devices

[17,18], it is necessary to find a few micrometer scaled MC waveguides having wide band gaps (a few GHz) for dipolar-exchange spin-waves (DESWs) in laterally confined planer structures.

In this Letter, we propose a new type of MC waveguides of a simple planar-patterned thin-film nanostrip in which magnonic bands of DESW and wide-band gaps of the order of 10 GHz can be manipulated by a means of the periodic modulation of different widths (a few tens of nm). The relations of the allowed DESW modes and their band gaps to the geometric variation of the proposed MCs were found from micromagnetic numerical and analytical calculations.

We performed micromagnetic simulations of DESW propagations in magnetic thin-film nanostrips. We used, as a model system, 10 nm-thick Py nanostrips of different widths (24 and 30 nm) modulating with a periodicity P ranging from 12 to 42 nm [light gray -colored area in Fig. 1(a)], which were connected directly to a segment of the Py nanostrip of 10 nm thickness and 30 nm width [yellow-colored area in Fig. 1(a)]. The unit period of the nanostrips consists of the same Py segments with different widths of 24 and 30 nm and with the corresponding lengths P_1 and P_2 , respectively, as illustrated in Fig. 1(b). The OOMMF code [19] was used to numerically calculate dynamics of \mathbf{M}_s of individual unit cells (size: $1.5 \times 1.5 \times 10 \text{ nm}^3$) interacting through exchange and dipolar forces, which code uses the Landau-Lifshitz-Gilbert equation of motion [20] valid for temporal scales above 10 ps. The chosen material parameters corresponding to Py are as follows: the saturation magnetization $M_s = 8.6 \times 10^5 \text{ A/m}$, the

exchange stiffness $A_{\text{ex}} = 1.3 \times 10^{-11}$ J/m, the damping constant $\alpha = 0.01$, the gyromagnetic ratio $\gamma = 2.21 \times 10^5$ m/As, and with the zero magnetocrystalline anisotropy. For the local excitation and subsequent propagation of the lowest DESW mode in the width direction (the y -axis), so called plane-wavelike mode in a frequency range of $f_{\text{SW}} = 0 \sim 100$ GHz, we applied a “sine cardinal (sinc)” function, denoted as $H_y(t) = H_0 \frac{\sin[2\pi\nu_{\text{H}}(t-t_0)]}{2\pi\nu_{\text{H}}(t-t_0)}$ with $H_0 = 1.0$ T and the field frequency $\nu_{\text{H}} = 100$ GHz in the local area of 1.5×30 nm² indicated by the dark-brown color in Fig. 1(a).

We plot the results obtained by the fast Fourier transform (FFT) of the temporal M_z/M_s evolution along the x -axis at $y = 15$ nm [18], as seen in Fig. 2. The frequency spectra clearly visualize the allowed and/or forbidden bands of the DESWs propagating through nanostrips: the allowed bands are indicated by the colored region, and the forbidden bands, by the blanked white region. For comparison, the fundamental DESW modes propagating in single-width (24 and 30 nm) nanostrip waveguides are shown in Figs. 2(a) and 2(b). Obviously, there is no forbidden band except for the intrinsic potential barrier (14 GHz), owing to the quantization of the lowest DESW mode by the geometric confinement of the narrow strip width [18,21]. For the nanostrips with different width modulation, by contrast, it is found that there are several wide forbidden bands of the order of ~ 10 GHz. Moreover, the number of forbidden bands as well as the bands’ position and gap width differ according not only to P but also the motif (represented by P_1/P). For example, for $P = 18$ nm ($[P_1, P_2] = [9$ nm, 9 nm]), there are two wide band gaps (11 and 16 GHz) in the DESW modes ranging from 14 to 100 GHz, whereas, for $P = 30$ nm ($[P_1,$

$P_2] = [15 \text{ nm}, 15 \text{ nm}]$), there are five forbidden bands with smaller gap widths (3.8 ~ 8.6 GHz) (For more data, see Suppl. Fig. 1 [22]).

To comprehensively understand such striking band-gap variations, we plot the dispersion curves of the DESW modes in the 24 and 30 nm-wide nanostrips and in the nanostrips of the width modulation of $[P_1, P_2] = [9 \text{ nm}, 9 \text{ nm}]$ [23] as an example. Due to the pinning of the DESWs at the edges of the nanostrip width, there exist certain width-modes having quantized k_y values [21]. Generally, in single-width nanostrips, several width-modes are excited and, thus, several concave branches are shown in the dispersion curves [18]. In the present simulation, however, there is a single parabolic dispersion curve, as shown in Fig. 3(a), because our employed homogeneous DESW excitations along the width axis lead to only the lowest mode having the smallest k_y value [the plane-wavelike mode, see Fig. 1(c)]. Accordingly, one would expect that the dispersion curves as for the width-modulated nanostrips are folded and have band gaps at the Brillouin zone (BZ) boundaries, similar to those found typically in a 1D periodic system [2,24]. However, the dispersion curves of the width-modulated nanostrip of $[P_1, P_2] = [9 \text{ nm}, 9 \text{ nm}]$ [Fig. 3(b)] show fairly complicated band features: The band gaps occur not only at the BZ boundaries, $k_x = n\pi/P$ with integers n (black dashed lines), but also at certain k values, $k_x = [(2n+1)\pi \pm 1.44]/P$ (red dotted lines). The former can be explained by a periodic translation symmetry associated with the width modulation along the DESW propagation direction, but the latter could not be understood by such 1D approach.

In order to elucidate quantitatively the physical origin of such different band gaps varying with different strip-width modulation, we compare magnonic band diagrams [the thick black lines in Fig. 4 (a)] numerically obtained from micromagnetic simulations for $[P_1, P_2] = [9 \text{ nm}, 9 \text{ nm}]$, combined with the analytical calculation of the band structure of a single width (27 nm) nanostrip. Note that this width is the average of the different widths of 24 and 30 nm used in the width-modulated nanostrips. For a single-width nanostrip, the dispersion relation can be approximately expressed as [18,21]

$$\omega_m^2(k_x) = \left[\omega_H + \omega_M L_e^2 \kappa_m^2 + \omega_M f(\kappa_m L) k_{y,m}^2 / \kappa_m^2 \right] \left[\omega_H + \omega_M L_e^2 \kappa_m^2 + \omega_M \{1 - f(\kappa_m L)\} \right] \quad (1)$$

with $f(\kappa_m L) = 1 - [1 - \exp(-x)]/x$, where $\omega_H = \gamma H_{\text{in}}$ with internal field H_{in} , $\omega_M = 4\pi\gamma M_s$, $L_e = \sqrt{A_{\text{ex}}/(2\pi M_s^2)}$ is the exchange length, and $\kappa_m^2 = k_x^2 + k_{y,m}^2$ is the in-plane-wave vector. The quantized $k_{y,m}$ can be obtained by considering the ‘‘effective’’ pinning [18,21] for a given single-width nanostrip, for example, $k_{y,m} = m \times 0.072 \text{ nm}^{-1}$ for a 27 nm-width nanostrip. In Fig. 4(a), the solid red-colored line indicates the dispersion curves of the DESW mode with $m = 1$, the lowest mode excited. Because of the periodicity of width modulation the dispersion curves are folded at the first BZ boundary (the dashed vertical line), as shown in Fig. 4(a) and thus, these folded branches intersect with the original one at the BZ boundaries. Such a crossing of dispersion curves indicates the ‘diagonal’ coupling between the two identical modes but with opposite propagation vectors [25], i.e., it denotes the interference between the initially propagating forward mode and backward mode reflected at the BZ boundary. This diagonal

coupling results in the formation of standing wave pattern of DESWs with $k_x = n\pi/P$ in the MC of P and yields a split in energy band (band gap) [see the thick black lines in Fig. 4(a)] [24].

To obtain the standing wave profiles near each band edge, we calculated the spatial distributions of the FFT powers of the local M_z/M_s oscillations for the indicated specific frequencies selected at the top and bottom of the magnonic band for the case of $[P_1, P_2] = [9 \text{ nm}, 9 \text{ nm}]$, as shown in Fig. 4(b). From the FFT profiles for the first band gap [26], it was clearly verified that the origin of the first band gap is the plane-wavelike standing wave modes [see the cross-sectional profile in Fig. 4(c)], originating from the diagonal coupling between the two identical but oppositely propagating lowest DESW modes ($m = 1$).

Since the multiple 2D scattering (diffraction) of SWs from the short-width edge steps [see Fig. 1(b)], the higher-quantized modes ($m = 3, 5, 7 \dots$) [27] can also be excited, although we generated, by applying the homogeneous field in the width direction (y -axis), only the plane-wavelike DESW having the first quantized wave vector ($m = 1$) in the 30 nm-width segment of the width-modulated nanostrip. The dotted orange lines in Fig. 4(a) indicate the dispersion curves of the DESW mode with $m = 3$, which are also folded at the first BZ boundary. Interestingly, this dispersion branch of the higher quantized mode ($m = 3$) excited by the DESW diffraction intersects with that of the lowest mode ($m = 1$) at a certain k value away from the BZ boundary [$k_x = [0.5 \pm 0.2]2\pi/P$ indicated by the blue circles and the arrows in Fig. 4(a)]. Such an intersection may have a remarkable influence on the propagating DESW modes. In general,

SWs scattered from the short-width edge steps propagate in the wide direction on the x - y plane, so that they interfere destructively with themselves. However, for the phase-matching condition of the diffracted SWs indicated by the intersection points in the dispersion curves shown in Fig. 4(a), these scattered SWs interfere constructively with themselves; in other words, another SW mode ($m = 3$) being propagating in the opposite direction are excited and it interacts with the initial propagating mode. Consequently, their interactions lead to quite complicated 2D standing SW modes (for $f_{\text{SW}} = 66.8$ GHz, nodes appear in the width direction (y -axis) and along the x -axis [see Figs. 4(b) and 4(c)]) analogues to complex 2D normal modes in thin films with lateral confinements [28] and result in the anti-crossing of dispersion curves as well as band gaps [25] [See the thick black lines for the second and the third bands and the diagonal-line patterned blue region between them in Fig. 4(a)]. Such strong couplings between the two different modes and resulting band gaps are well known as ‘mini-stopbands’ [2,25,29]. in the case of electromagnetic waves in photonic crystal waveguides.

On the basis of such novel band structures of DESWs, it was found that magnonic band gaps vary sensitively with both the periodicity and motif in strip-width-modulated nanostrips, as seen in Suppl. Fig.2 [22]. From an application point of view, this novel property can be implemented as an effective means of manipulating the allowed DESWs modes in their propagations through such width-modulated nanostrip waveguides. Here, we propose a new type of SW waveguide that passes DESWs in a chosen narrow-band frequency but filters out most of

DESWs with the other frequencies. The proposed width-modulated planar structure, as shown in Fig. 5(a), consists of four different nanostrip segments of different strip-width modulations, and different periodicities and repeating numbers. These serially combined nanostrips were designed for passing SWs in the narrow band of 26 ~ 32 GHz, based on the results of the variations of the band gaps with P and P_1 (see Suppl. Fig. 2). From the frequency spectrum [Fig. 5(b)], and the transmitted intensity of the DESWs versus the propagation distance [Fig. 5(c)], the DESWs of a narrow frequency range of 26 ~ 32 GHz propagate well with a transmitted intensity of about 10% even after distance as long as 1.5 μm , indicating that such MC structures effectively filter out most SWs except for a chosen SW mode. Another example of a narrow-band SW filter, having a 36 ~ 41 GHz pass band, is shown in Suppl. Fig. 3 as well [22].

In conclusion, we have found that a new type of MCs of the periodic modulation of different strip widths yields complex DESW band structures and wide band gaps, originating from the coupling between two identical as well as between different modes in width-modulated nanostrips. Moreover, we propose promisingly efficient magnonic crystal waveguides of a simple patterned planar structure of nanostrips that are serially connected with different-width-modulated nanostrip segments but made of a single material, for narrow-band-pass DESWs retaining ~ 10% transmission intensity after having traveled distances as long as ~ 1 μm . The magnonic band-gap width, the position, and the number of the band gaps are controllable by means of the periodicity and the motif of the strip-width modulation. This work paves the way

for effective manipulation of magnonic bands and band gaps of DESWs in the GHz range, providing a route for realizing a promisingly efficient spin-wave filter using a simple planar-patterned thin-film structure from a single magnetic material.

This work was supported by Creative Research Initiatives (the Research Center for Spin Dynamics and Spin-Wave Devices) of MEST/KOSEF.

References:

* corresponding author, e-mail address: sangkoog@snu.ac.kr

- [1] E. Yablonovitch, Phys. Rev. Lett. **58**, 2059 (1987).
- [2] J. D. Joannopoulos, R. D. Meade, and J. N. Winn, Photonic Crystals: Molding the Flow of Light, 2nd ed. (Princeton University, Princeton, NJ, 2008).
- [3] N. Engheta, Science **317**, 1698 (2007).
- [4] R. L. Carter *et al.*, J. Appl. Phys. **53**, 2655 (1982).
- [5] D. S. Deng, X. F. Jin, and R. Tao, Phys. Rev. B **66**, 104435 (2002).
- [6] S. A. Nikitov, Ph. Tailhades, and C. S. Tsai, J. Magn. Magn. Mater. **236**, 320 (2001).
- [7] M. P. Kostylev, A. A. Stashkevich, and N. A. Sergeeva, Phys. Rev. B **69**, 064408 (2004); M. Kostylev *et al.*, Appl. Phys. Lett. **92** 132504 (2008).
- [8] C. G. Sykes, J. D. Adam, and J. H. Collins, Appl. Phys. Lett. **29**, 388 (1976); P. A. Kolodin and B. Hillebrands, J. Magn. Magn. Mater. **161**, 199 (1996).
- [9] A. V. Chumak *et al.*, Appl. Phys. Lett. **93**, 022508 (2008);.
- [10] H. Al-Wahsh *et al.*, Phys. Rev. B **59**, 8709 (1999).
- [11] A. Mir *et al.*, Phys. Rev. B **64**, 224403 (2001).
- [12] J. O. Vasseur *et al.*, Phys. Rev. B **54**, 1043 (1996).
- [13] Yu. V. Gulyaev *et al.*, JETP Lett. **77**, 567 (2003).

- [14] M. Krawczyk and H. Puzskarski, Phys. Rev. B **77**, 054437 (2008).
- [15] V.V. Kruglyak, and R.J. Hicken, J. Magn. Magn. Mater. **306**, 191 (2006); V.V. Kruglyak *et al.*, J. Appl. Phys. **98**, 014304 (2005).
- [16] C. Bayer, M. P. Kostylev, and B. Hillebrands, Appl. Phys. Lett. **88**, 112504 (2006).
- [17] R. Hertel, W. Wulfhekel, and J. Kirschner, Phys. Rev. Lett. **93**, 257202 (2004); T. Schneider *et al.*, Appl. Phys. Lett. **92**, 022505 (2008); K.-S. Lee and S.-K. Kim, J. Appl. Phys. **104**, 053909 (2008).
- [18] S. Choi, K.-S. Lee, K. Y. Guslienko and S.-K. Kim, Phys. Rev. Lett. **98**, 087205 (2007).
- [19] See <http://math.nist.gov/oommf>.
- [20] L. D. Landau and E. M. Lifshitz, Phys. Z. Sowjet. **8**, 153 (1935); T. L. Gilbert, Phys. Rev. **100**, 1243A (1955).
- [21] K. Yu. Guslienko *et al.*, Phys. Rev. B **66**, 132402 (2002); K. Yu. Guslienko and A. N. Slavin, Phys. Rev. B **72**, 014463 (2005).
- [22] See EPAPS Document No. XXX for two movie files. For more information on EPAPS, see <http://www.aip.org/pubservs/epaps.html>.
- [23] Dispersion curves were obtained from the 2D FFTs of the temporal M_z/M_s oscillations along the x -axis ($x = 501 \sim 1500$ nm) at $y = 15$ nm (dashed line on the nanostrpe MC in Fig. 1).
- [24] C. Kittel, Introduction to Solid State Physics, 7th ed. (Wiley, New York, 1996).

[25] J.-M. Lourtioz *et al.*, Photonic Crystals: Towards Nanoscale Photonic Devices (Springer, Berlin, 2005).

[26] The top of the first allowed band ($f_{\text{sw}} = 25.6$ GHz) and the bottom of the second allowed band ($f_{\text{sw}} = 36.4$ GHz) appear at the edge of the Brillouin zone at $k_x = \pi/P$.

[27] Since the edge steps are symmetric with respect to the x -axis (mirror plane), higher-quantized modes have a mirror symmetry in the profiles along the short-width axis; in other words, they have an odd number of m values (i.e., $m = 3, 5, 7, \dots$).

[28] M. Grimsditch *et al.*, Phys. Rev. B **69**, 174428 (2004); M. Grimsditch *et al.*, Phys. Rev. B **70**, 054409 (2004).

[29] S. Olivier *et al.*, Phys. Rev. B **63**, 113311 (2001).

Figure captions

FIG. 1. (online color) (a) Geometry and dimensions of proposed nanostrip magnonic crystals with the periodic modulation of different strip widths. The initial \mathbf{M}_s point in the $-x$ direction, as indicated by the black arrow. The dark-brown and yellow areas indicate the SW generation part and the waveguide component for SW propagation, respectively. (b) The unit period of $P = P_1 + P_2$, where P_1 and P_2 are the segment lengths of 24 and 30 nm widths, respectively. (c) Temporal evolution of the spatial M_z/M_s distribution excited by the “sinc” function field with $H_0 = 1.0$ T applied along the y -axis to only the dark-brown area.

FIG. 2. (online color) Frequency spectra obtained from fast Fourier transform (FFT) of M_z/M_s oscillation along the x -axis at $y = 15$ nm, for single-width nanostrips of 24 and 30 nm and for MCs with different cases of $[P_1, P_2]$ as noted. The vertical dashed orange lines indicate the boundary between the single-width nanostrip waveguide [the yellow colored area in Fig. 1(a)] and the MC of width-modulated nanostrip [the light gray colored area in Fig. 1(a)].

FIG. 3. (online color) (a) Dispersion curves for DESWs propagating through single-width nanostrips of 24 and 30 nm as noted. (b) Dispersion curves of DESWs existing in the MCs with $[P_1, P_2] = [9 \text{ nm}, 9 \text{ nm}]$ within nanostrip area only, from $x = 500$ to 1500 nm, obtained from FFTs of the temporal M_z/M_s oscillations along with the x -axis at $y = 15$ nm. The black dashed

lines indicate the Brillouin zone boundaries $k = n\pi/P$, where $n = 0 \pm 1, \pm 2, \dots$, and the red dotted lines denote certain k values, $k_x = (2n+1)\pi/P \pm 0.08$ at which the forbidden band gaps occur.

FIG. 4. (online color) (a) Comparison of magnonic band structure (black thick curves) of nanostrip-type MC of $[P_1, P_2] = [9 \text{ nm}, 9 \text{ nm}]$ obtained from micromagnetic simulations and that of single-width nanostrips of 27 nm width, for two different modes of $m = 1$ (solid red) and 3 (dotted orange). (b) Perspective view of FFT power distributions of local M_z/M_s oscillations for specific frequencies for the top and bottom of allowed bands, as indicated by orange horizontal lines in the dispersion curves shown in Fig. 3(b). (c) Cross-sectional FFT power profiles of standing wave modes in width direction (y -direction). The red (green) line indicates the standing wave mode profile in the width direction at the center of the 30 nm- (24 nm-) wide segment.

FIG. 5. (online color) (a) Proposed wide-band SW filter in GHz range having only pass band of 26 ~ 32 GHz, and composed of four different strip-width modulations, each of which is represented by $[P_1 \text{ (nm)}, P_2 \text{ (nm)}] = [21, 21], [13.5, 13.5], [12, 12],$ and $[7.5, 7.5]$ in present case. (b) Frequency spectra along long axis (x -axis) of nanostrip. The vertical lines separate the different period modulations. (c) FFT power profiles along long axis (x -axis) of nanostrip for different frequencies as noted.

FIG.1

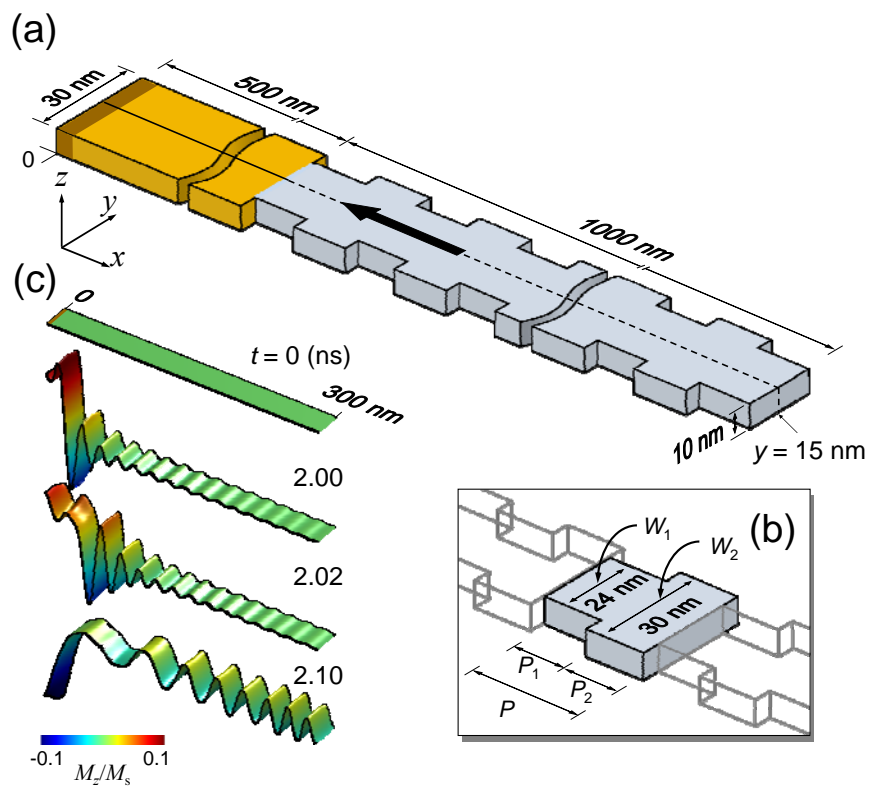


FIG.2

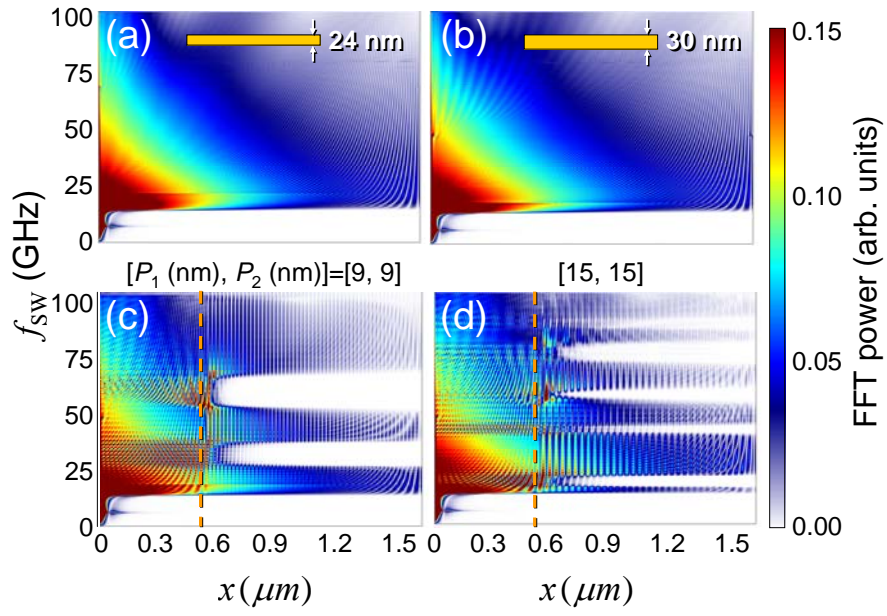


FIG.3

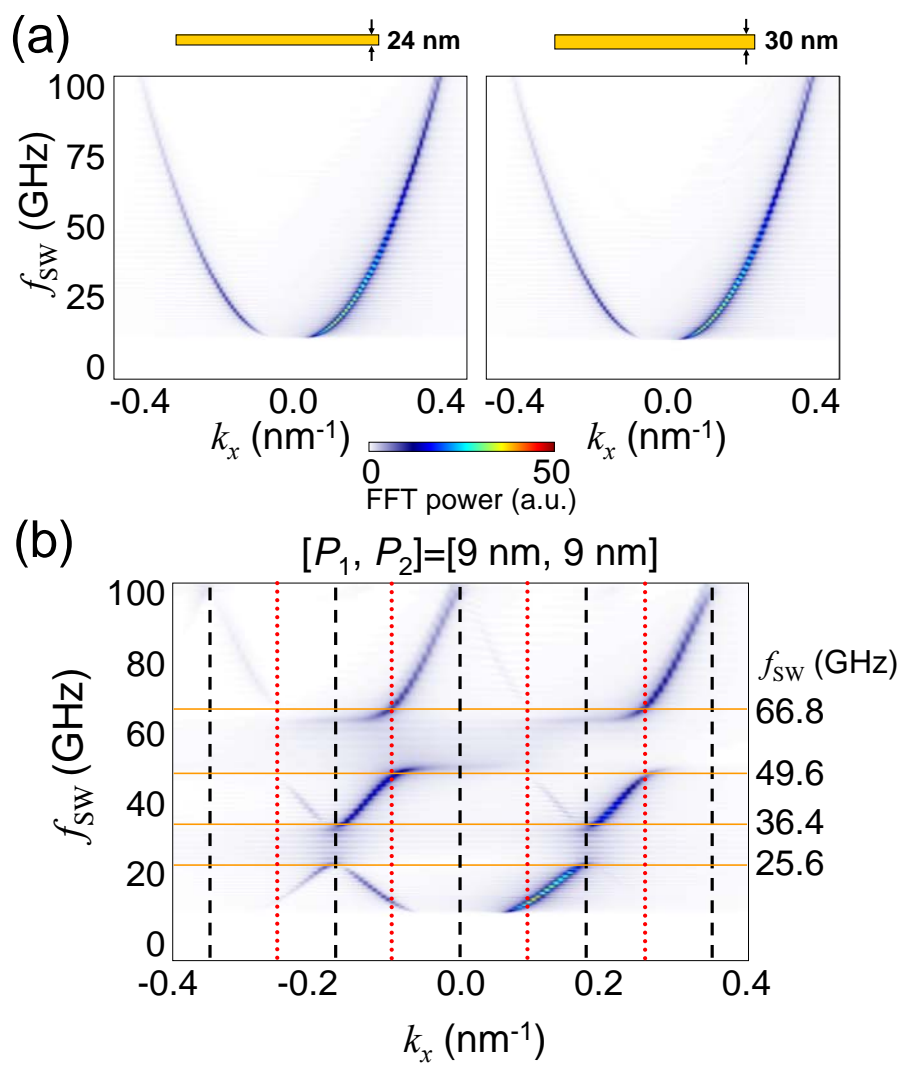


FIG.4

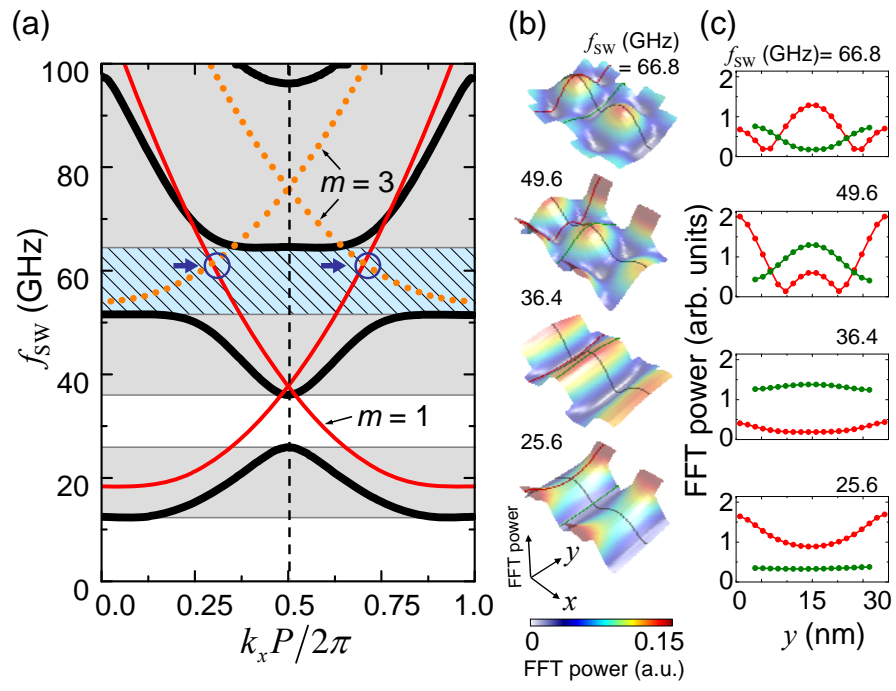
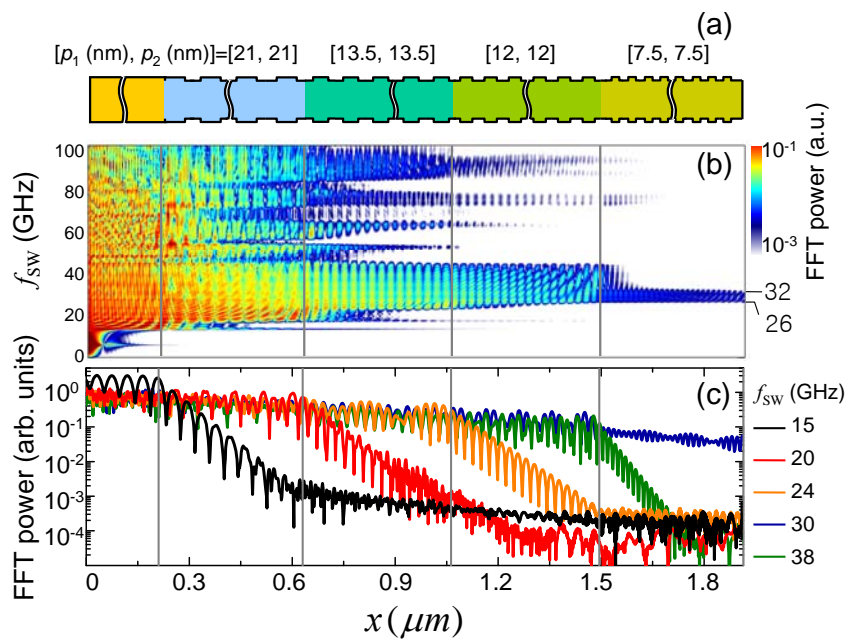


FIG.5

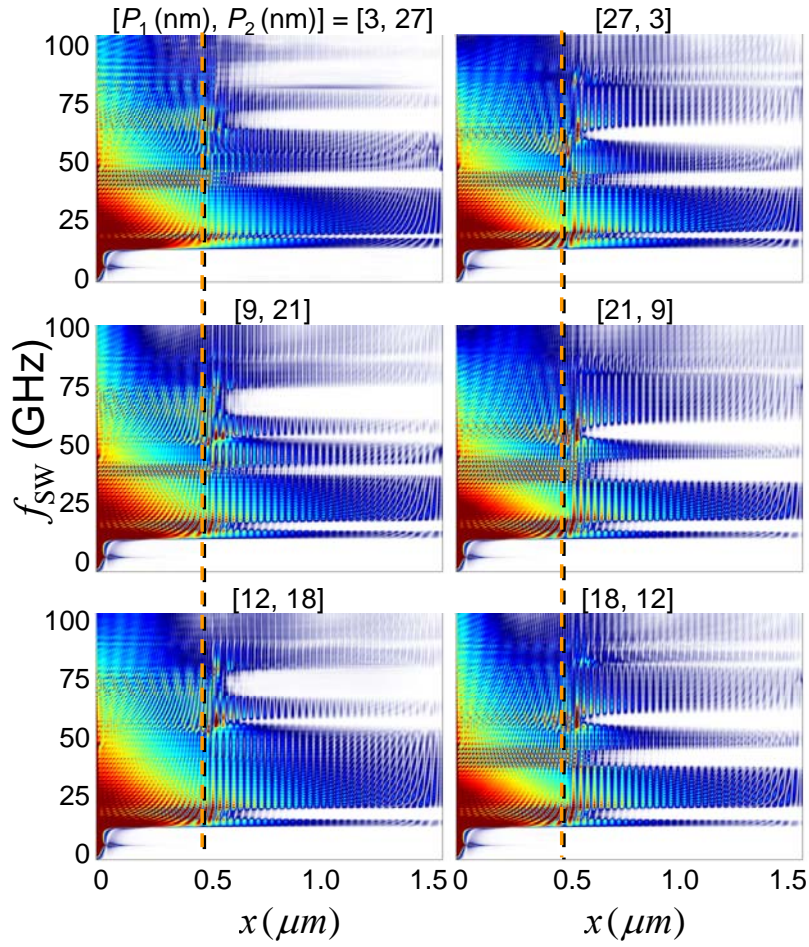


Supplementary Documents

Variation of the allowed and forbidden bands according to the periodicity P and the motif represented by P_1/P

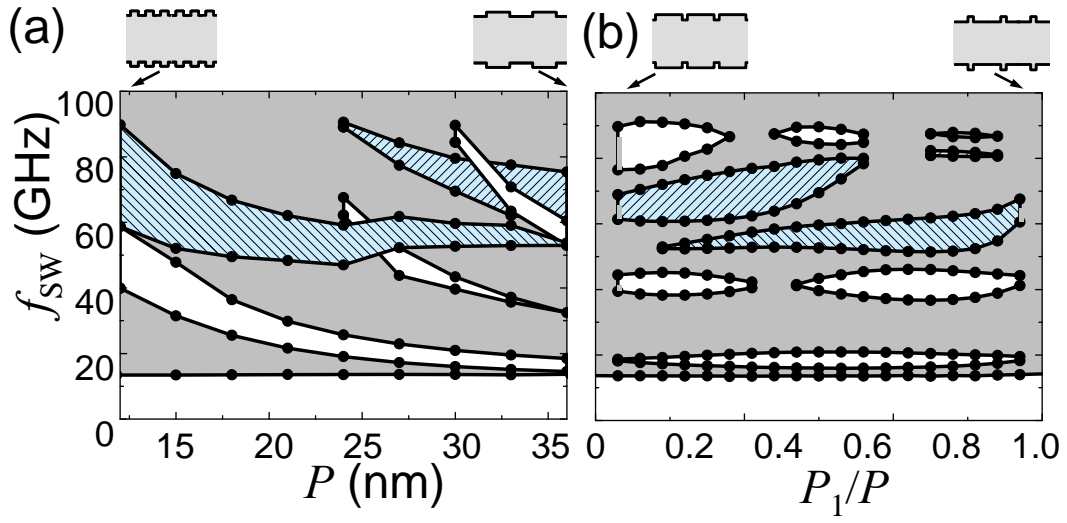
To examine the variation of the allowed and forbidden bands in a nanostrip type magnonic crystals (MCs) according to the periodicity $P = P_1 + P_2$ and the motif represented by the relative segment length, P_1/P , we obtained frequency spectra along the x -axis for various value of P_1 and P_2 as shown in Suppl. Fig. 1. From these data, the magnonic band gaps were plotted versus P while retaining $P_1 = P_2$ in Suppl. Fig. 2(a), and versus P_1/P with the constant value of $P = 30$ nm in Suppl. Fig. 2(b). All of the gray regions indicate the allowed bands, whereas the white and blue regions indicate the forbidden bands at the zone boundary and at a certain k value away from the zone boundary, respectively. As seen in Suppl. Fig. 2(a), the number of the band gaps as well as the center positions and widths of the individual gaps change dramatically with P . For the forbidden bands at the zone boundaries (the white regions), the center position and width of each band decrease with increasing P , whereas the center positions do not change with P_1/P . By contrast, for the forbidden bands occurring away from the zone boundary (the blue region), their center positions change with both of P and P_1/P .

SUPPL. FIG. 1



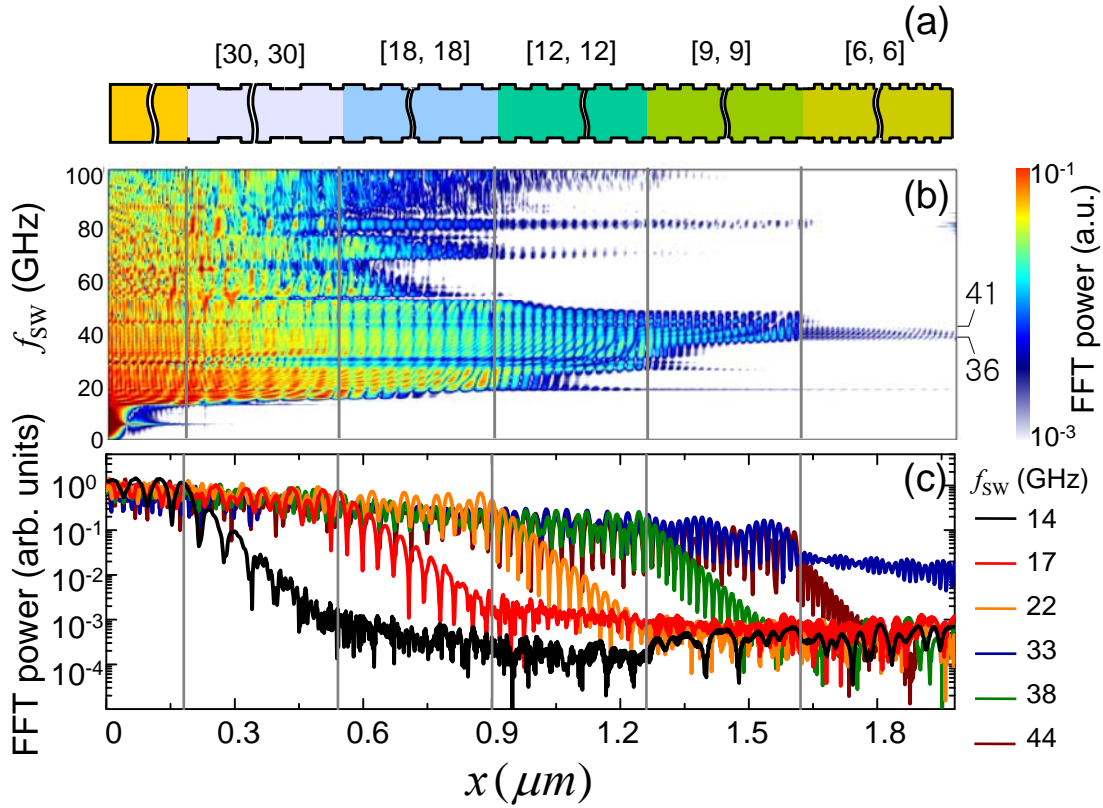
SUPPL. FIG. 1. Frequency spectra obtained from fast Fourier transform (FFT) of M_z/M_s oscillation along the x -axis at $y = 15$ nm, for cases of the same $P = 30$ nm but different P_1/P_2 values as noted. The vertical dashed orange lines indicate the boundary between the single-width nanostrip waveguide (the yellow colored area in Fig. 1) and the MC of width-modulated nanostrip (the light gray colored area in Fig. 1).

SUPPL. FIG. 2



SUPPL. FIG. 2. Allowed and forbidden bands according to P for case of $P_1 = P_2$ in (a) and P_1/P , maintaining $P = P_1 + P_2 = 30$ nm in (b). The gray area indicates the allowed bands, whereas the white (blank) and blue (diagonal-line pattern) areas indicate the forbidden bands at the Brillouin zone boundary $k = n\pi/P$, where $n = 0, \pm 1, \pm 2, \dots$, and certain k values, $k \neq n\pi/P$, respectively.

SUPPL. FIG. 3



SUPPL. FIG. 3. (a) Proposed wide-band SW filter in GHz range having only pass band of 36 ~ 41 GHz, and composed of four different strip-width modulations, each of which is represented by $[P_1$ (nm), P_2 (nm)] = [30, 30], [18, 18], [12, 12], [9,9], and [6, 6] in present case. (b) Frequency spectra along long axis (x -axis) of nanostrip. The vertical lines separate the different period modulations. (c) FFT power profiles along long axis (x -axis) of nanostrip for different frequencies as noted.